A new spent coffee grounds based biochar - persulfate catalytic system for enhancement of urea removal in reclaimed water for ultrapure water production

Yuanying Yang[a,b], Xinbo Zhang[a,b,*], Huu Hao Ngo[a,c,*], Wenshan Guo[a,c], Zening Li[a,b], Xiao Wang[d], Jianqing Zhang[d], Tianwei Long[a,b]

[a]*Joint Research Centre for Protective Infrastructure Technology and Environmental Green Bioprocess, School of Environmental and Municipal Engineering, Tianjin Chengjian University, Tianjin 300384, China*

[b]*Tianjin Key Laboratory of Aquatic Science and Technology, Tianjin Chengjian University, Jinjing Road 26, Tianjin 300384, China*

[c]*Centre for Technology in Water and Wastewater, School of Civil and Environmental Engineering, University of Technology Sydney, Sydney, NSW 2007, Australia*

[d]*TG Hilyte Environment Technology (Beijing) Co., LTD., Beijing 100000, China*

* Correspondence authors: Email: zxbcj2006@126.com (X. B. Zhang);

ngohuuhao121@gmail.com (H. H. Ngo)

Abstract

The demand for ultrapure water (UPW) in the semiconductor industry has increased in recent years, while the idea to use reclaimed water instead of tap water for UPW production has also attracted more attention. However, since urea concentration in reclaimed water is higher than that in tap water, UPW production has not been efficient. To resolve this problem, this study aims to develop a new spent coffee grounds based biochar (SCG-BC) /persulfate catalytic system as a pretreatment unit. The objective is to enhance urea removal from reclaimed water so that UPW production is more effective. In this study, the biochar used was prepared from spent coffee grounds with detailed characterization. Results strongly suggested that the urea removed by SCG-BC /persulfate catalytic system was very encouraging (up to 73%). The best possible dosages for SCG-BC and persulfate for urea removal were 0.2 and 2.0 g L^{-1}, respectively. Furthermore, this system could remove urea effectively in a wide range of pH (3-10). Moreover, the characterizations of SCG-BC (graphite C, defective edges and functional groups, i.e. -OH, C=O, carboxyl C-O) helped to activate persulfate in the catalytic process. $OH^{\bullet}$ and $SO_4^{\bullet -}$ were all involved in this process, while the $SO_4^{\bullet -}$ was the main radical for urea degradation.

Keywords: Ultrapure water; Urea; Biochar; Advanced oxidation processes; Persulfate activation

1. Introduction

With the continuous acceleration of the worlds' urbanization and rapid, unchecked growth of populations, shortages of potable water resources have become a serious and long-lasting problem. Consequently, promoting unconventional water resources reclamation and/or utilization is viable for the required level of sustainable economic development (Guo et al., 2014; Cheng et al., 2017). At present, due to the booming semiconductor industry, the demand for ultrapure water (UPW) is rising in this particular sector of the economy. The idea to use reclaimed water for producing UPW is acceptable in terms of raw water demand and sustainable usage of water resources (Zhang et al., 2021). Some studies have confirmed the feasibility of applying municipal sewage as raw water to produce UPW (Lefebvre, 2018; Wang et al., 2019). For instance, Singapore's NEWater is high-grade reclaimed water and it is produced from municipal wastewater through membrane technology and ultraviolet (UV) irradiation (Lefebvre, 2018; Wang et al., 2019). It can be used in industries where the requirements for UPW do not demand high quality. However, UPW is commonly employed for wafer cleaning in the semiconductor industry, and the range of water purity is defined in accordance with the manufacturing process. For instance, Type E-1.2 (18.2 MΩ cm, TOC <1 μg L^{-1}) is used in production of devices with line widths between 0.065 and 0.032 μm and Type E-1.1 (18.2 MΩ cm, TOC <2 μg L^{-1}) for 0.09 and 0.18 μm according to the American Society of Testing and Materials (ASTM) D5127-13 (2018) (ASTM, 2018). Therefore, UPW quality does play a vitally important role in its preparation (Choi et al., 2016; Choi and Chung, 2019).

The UPW effluent quality affects whether a defective product incident does occur (Zhao et al., 2019). Previous studies have found that urea resulted in the TOC concentrations exceeding the limit in UPW (Rydzewski and Godec, 2002; Choi and Chung, 2019). Recently,

Choi and Chung (2019) proved it through one-year monitoring of urea and TOC concentrations in the effluent in real-life UPW production (Choi and Chung, 2019). It is difficult to remove urea with conventional UPW treatment techniques, such as ion exchange, reverse osmosis (RO), granular activated carbon (GAC) adsorption, and UV irradiation, due to its high solubility in water, low molecular weight and no surface charge. These results in excessive TOC in UPW effluent (Choi and Chung, 2019). Of the above-noted methods, GAC can remove most macromolecules effectively without polarity, but it is hard to remove small molecules which are easily soluble, such as urea (Schmotzer et al., 2002; Sun and Chen, 2014; Zhang et al., 2021). RO is an indispensable process for UPW production to remove small amounts of molecular organics. Unfortunately, the rejection rate of urea via RO was very low ranging from 20% to 50% in two studies (Yoon and Lueptow, 2005; Singh, 2016). This is mainly due to the fact that urea is a small uncharged molecule, so it cannot be eliminated by charge repulsion or size repulsion. In addition, UV radiation can remove most organics in water, but the maximum amount of urea removed is less than 10% (Choi and Chung, 2019; Zhang et al., 2021) because the N-bonds in urea cannot be destroyed by UV (Singh, 2016).

Recently, persulfate technology is regarded as one of the latest advanced oxidation processes (AOPs) being investigated in the world to degrade organic pollutants in water and wastewater (Ghauch et al., 2017; Al Hakim et al., 2019; Al Hakim et al., 2020; Yao et al., 2021a; Yao et al., 2021b). Sulfate radical-based AOPs have garnered increasing interest due the sulfate radicals' ($SO_4^{\bullet -}$) remarkable redox potential (E^0 = 2.5-3.1 V) and long half-lifetime (30-40 μs) (Dong et al., 2017; Duan et al., 2018; Zhou et al., 2020). Furthermore, persulfate can directly eliminate some organic compounds without using radical species (Ding et al., 2021). Recent studies have identified that any methods that can enhance the oxidation ability of persulfate,

whether involving radicals, are considered to be "persulfate-AOPs" (Yang et al., 2018; Lee et al., 2020a). Currently, persulfate-AOPs have been incorporated into the UPW production process because it can effectively degrade urea in water (Singh, 2016; Choi and Chung, 2019). In these studies, persulfate was activated by UV irradiation and urea was oxidized by numerous $SO_4^{\bullet -}$. However, a UV dosage 12 times higher than normal was needed to achieve a high removal of urea (about 90%), which subsequently greatly increased the operating costs (Choi and Chung, 2019). Moreover, the raw water used in these studies was not reclaimed water, and the desired removal outcomes cannot be guaranteed when the raw water quality deteriorates.

Activation method is crucial in a persulfate activation system. Although metals and their oxide catalysts reveal superior catalytic functioning for persulfate activation, serious toxic metal leaching and poor stability limit their extensive application (Hu and Long, 2016; Yu et al., 2019). The persulfate activation by UV, ultrasonic or heat requires an external energy supply, resulting in higher cost (Oh et al., 2016). Recently, typical carbon materials represented by carbon nanotubes (Ren et al., 2019), graphene (Chen et al., 2018), nano-diamonds (Shao et al., 2018) and biochar (Zhang et al., 2020b) have emerged as viable alternative materials in persulfate catalysis (Ding et al., 2021). Carbonaceous-based materials are effective catalysts and they do not require an external energy supply while metal leaching can be avoided (Oh et al., 2016). Among them, biochar produced by pyrolysis of waste biomass has the advantage practical application at low cost (Xiu et al., 2017).

Along with current and expanding explorations of biochar, spent coffee grounds have attracted much interest for their practical applications (Nguyen et al., 2019a, 2019b). In this research paper, spent coffee grounds were used as biochar precursor to decompose urea efficiently in a persulfate catalytic system for the first time. The main objectives of this study

were to: (i) prepare and characterize spent coffee grounds biochars; (ii) explore the urea adsorption capacity of spent coffee grounds biochars; (iii) estimate the effect of the catalytic system on urea removal and explore the catalytic mechanism; and (iv) investitage the influence of pH, biochar dosage and persulfate dosage on the degradation of urea. This paper is expected to provide an viable and practical technology that can enhance the current UPW production system.

2. Materials and methods

2.1. Materials

Spent coffee grounds were collected from a café in Tianjin. Urea (analytical grade, 99%) was purchased from Shanghai Yuanye Bio-Technology Co., Ltd (Shanghai, China). 2,3-Butanedione monoxime (analytical grade, 99%), antipyrine (analytical grade, 99%) and sodium persulfate ($Na_2S_2O_8$, analytical grade, 99%) were obtained from Shanghai Macklin Biochemical Share Co., Ltd. (Shanghai, China). Sulfuric acid (analytical grade, 98%), Methanol (MeOH, analytical grade, 99%) and tert-butanol (TBA, analytical grade, 99%) and acetic acid (analytical grade, 36%) were purchased from Tianjin Jindongtianzheng Precision Chemical Reagent Factory (Tianjin, China). All reagents or chemicals employed in this research were used directly without further purification. The aqueous urea solutions involved in the experiments were prepared using UPW produced in the laboratory (resistivity ≈18.2 MΩ cm).

2.2. Preparation of spent coffee grounds based biochar (SCG-BC)

The waste coffee grounds collected were firstly put in an oven at 110 °C and dried to achieve a constant weight. After grinding, the spent coffee grounds were calcined in a muffle

furnace at 900 °C, which was operated for 2 h under limited oxygen conditions. The pyrolysis heating rate was 5 °C min^{-1} and the obtained black material was spent coffee grounds, labeled as SCG-BC. Further screening all samples was done with a 80-mesh sieve (≤0.18 mm) (Zhang et al., 2020b).

2.3. Characterization of SCG-BC

X-ray photoelectron spectrometry (XPS, K-alpha, USA) and Raman spectra (Renishaw inVia) helped to analyze the valence state of elements existing on the SCG-BC surface and structure of SCG-BC. Fourier transform infrared spectroscopy (FTIR, Is10, US) was used to examine the functional groups of SCG-BC. The surface area and total pore volumes of the SCG-BC were measured using the Brunauer-Emmett-Teller (BET) method.

2.4. Preliminary evaluation of urea removal

2.4.1. Catalytic activity experiments

In this study, urea was selected as the main target pollutant. Specifically, reaction solutions were prepared with urea in deionized water (1 mg L^{-1}). Secondly, the SCG-BC sample and 400 mL urea solution (1 mg L^{-1}) were collected in a 500 mL flask. After that, persulfate was added to induce the reaction and then the flask was placed in the shaker. The shaking rate was retained at 180 rpm for the purpose of uniform distribution. At given time intervals (10, 30, 60, 120, 180, 240 and 300 min), the reaction sample was extracted. The sample was then filtered through a 0.45 μm polyether sulfone (PES) membrane. In order to further explore the role of radicals, several radical scavengers were selected to inhibit the radical reaction. MeOH was used to scavenge $SO_4^{\bullet -}$ and $OH^{\bullet}$ and TBA was employed to scavenge $OH^{\bullet}$ (Ghauch et al., 2017).

Furthermore, the effect of persulfate and SCG-BC dosage was investigated. The initial

urea concentration was 1.0 mg L^{-1} and SCG-BC dosage was 0.2 g L^{-1}. After that, persulfate was added from 0.8 to 6 g L^{-1} to determine the effect of persulfate dosage. Similarly, the SCG-BC dosage varied from 0.05 to 0.8 g L^{-1} with the initial urea and persulfate concentrations being 1 and 2 g L^{-1}, respectively. Then the experiment procedures were conducted as stated above. All the tests were done in triplicate and the data expressed as the mean values.

2.4.2. Adsorption experiments

The adsorption experiments were performed at 25 □ with SCG-BC serving as the adsorbent. Firstly, a urea solution was prepared in deionized water (1 mg L^{-1}). Subsequently, the SCG-BC sample and 400 mL urea solution (1 mg L^{-1}) were put into a 500 mL flask, which was then placed in the shaker. The shaking rate was kept at 180 rpm for the uniform distribution and the reaction sample was extracted after 5 hours. Subsequently, the sample was filtered through a 0.45 μm polyether sulfone (PES) membrane. To determine the adsorption effect of SCG-BC dosage, SCG-BC with different dosages (0.05, 0.1, 0.2, 0.4 and 0.8 g L^{-1}) were employed. All the experiments were repeated in triplicate.

2.5. Determination of urea concentration

The urea concentration was analyzed using UV-Vis spectrophotometer (Shimadzu, UV-2600). Specifically, the 10 mL water sample was placed in a 25 mL brown tube and diluted to 25 mL with pure water. Subsequently, 1.0 mL 2,3-Butanedione monoxime (2%) and 2.0 mL antipyrine (0.2%) were put into the tube. After mixing, the samples were put into a boiling water bath for 50 min and then cooled in a tube filled by running tap water for 2 min. Following that the urea concentration was determined by UV at 460 nm.

3. Results and discussion

3.1. Characterization of SCG-BC

The specific surface area of SCG-BC was 315.5 $m^2 g^{-1}$ and the pore volume was 0.34 $cm^3 g^{-1}$. The large specific surface area could reinforce the adsorption of pollutants. It can promote the electron transfer process during catalysis (Dutta et al., 2014), which encouraged the catalytic reaction since it is known that carbon catalysts have two crucial characteristics peaks: D peaks (1320-1350 cm^{-1}) and G peaks (1570-1585 cm^{-1}) (Wang et al., 2012). Furthermore, the higher I_D/I_G (D peaks and G peaks intensity ratio) value indicates the higher level of disorder. As shown in Fig. 1a, SCG-BC had two major characteristic peaks at 1350 and 1595 cm^{-1}, respectively. The D peak at 1350 cm^{-1} in this work reflected the extent of disorder regarding SCG-BC (Ferrari and Robertson, 2000). Another G peak at 1595 cm^{-1} demonstrated the existence of graphitic carbon. In addition, the I_D/I_G value represents the intensity ratio of D peak and G peak, which was determined by calculating the peak area. Fig. 1a indicated that the I_D/I_G was 1.20 and the high temperature during pyrolysis may lead to defective edges appearing at the biochar boundaries (Keiluweit et al., 2010; Guizani et al., 2017). As well, the character of 2D near 2800 cm^{-1} showed that SCG-BC had the characteristic several-layered graphite structure. This may be due to the increasing temperature, which can lead to the phase transition from amorphous carbon to graphitized carbon (Liu et al., 2020; Zhou et al., 2020).

From the FTIR analysis of SCG-BC (Fig. 1b), the centered at 3441, 1636, 1380 and 675 cm^{-1} could be observed. The band at around 3441 cm^{-1} denoted the characteristic stretching of -OH, the peak at 1636 cm^{-1} was attributed to C=C or C=O, while the band at around 1380 cm^{-1} belonged to the vibration of carboxyl C-O. Furthermore, the aromatic C-H vibration is recognized at around 675 cm^{-1} (Hu et al., 2020b; Zhang et al., 2020a). Overall, the SCG-BC

prepared at 900 □ still retained a variety of functional groups, which may play a critical role in subsequent adsorption and catalytic reactions.

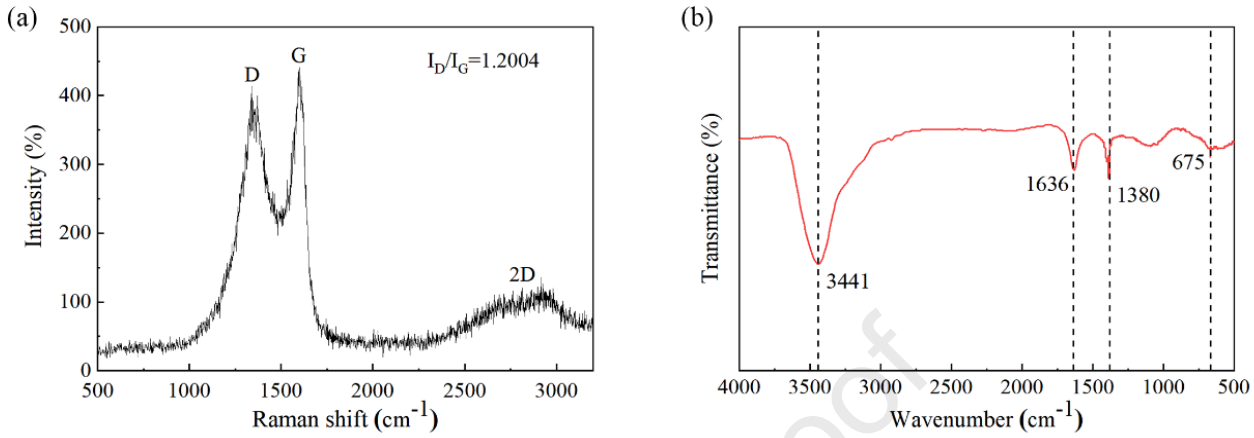

Fig. 1. (a) Raman spectra and (b) FTIR spectra of SCG-BC

3.2. Evaluation of urea removal

3.2.1. Urea removal by SCG-BC adsorption

In general, GAC is essential in the UPW system because it has a strong adsorption capacity. Pollutants such as suspended solids, ions and macromolecular organics in water can be removed by GAC in the pretreatment stage (Schmotzer et al., 2002). Compared with activated carbon, biochar is cheaper and can be obtained from waste products. It has recently shown considerable potential as a low-cost replacement material of GAC for eliminating contaminants (Oleszczuk et al., 2017; Xu et al., 2017; Zhu et al., 2019b). Furthermore, the removal effect of biochar on pollutants could be better than that of activated carbon in some cases (Ahmad et al., 2014; Huggins et al., 2016; Liang et al., 2019). For this reason, it is economical and feasible to choose biochar as an alternative material analogous to activated carbon in the pretreatment process required for UPW production. Meanwhile, the operational costs can be minimized or better controlled. On this basis the adsorption effect of SCG-BC when removing urea was initially

examined.

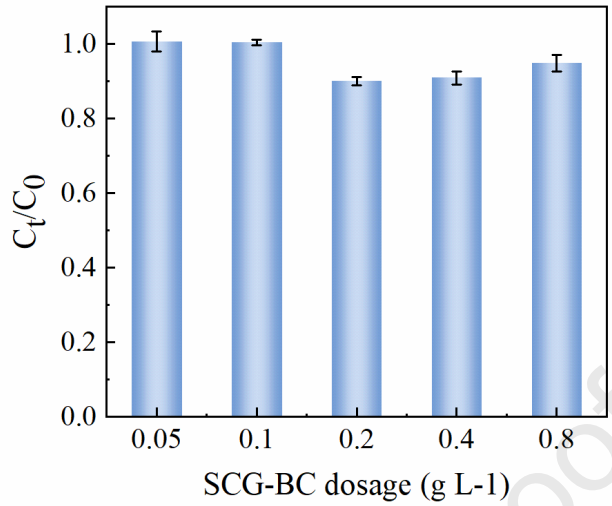

Fig.2. Efficiencies of urea removal using SCG-BC adsorption (C_0 represent the initial urea concentration (mg L^{-1}) in the solution; C_t represent the urea concentration (mg L^{-1}) in the solution after the degradation reaction.)

In the preliminary test the adsorption experiments were completed. As shown in Fig. 2, adding a small amount of SCG-BC (0.05, 0.1 g L^{-1}) could not remove urea. With the increase in the biochar dosage, the urea removal rate did improve to a certain extent. However, there was no further improvement in urea removal efficiency after the SCG-BC dosage exceeded 0.2 g L^{-1}. It was inferred that the adsorbed pollutants were released from the adsorbent into the water. It was also caused by the small concentration of urea as the urea concentration gradient between solution and adsorbent surface and mass transfer driving force were higher in the high urea concentration scenario (Liu et al., 2013). Clearly, adding biochar alone to remove urea was not ideal, and the best removal rate could only reach 11%. It is speculated that since biochar material had high hydrophobicity, its affinity for urea was low owing to the hydrophilic nature of urea (Mortazavian et al., 2019; Clurman et al., 2020; Nguyen et al., 2021; Zhang et al., 2021).

3.2.2. Urea removal by SCG-BC activating persulfate

Fig. 3 illustrates that SCG-BC can effectively activate persulfate and greatly improve the amount of urea removed in the catalytic system by as much as 73%.

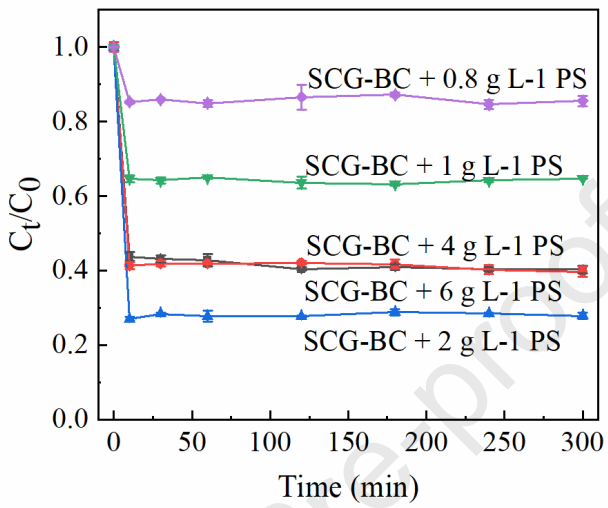

Fig. 3. Urea removal efficiencies in the catalytic system ([SCG-BC] 0.2 g L^{-1}, [urea] 1 mg L^{-1}; C_0 represent the initial urea concentration (mg L^{-1}) in the solution; C_t represent the urea concentration (mg L^{-1}) in the solution after the degradation reaction.)

The degradation of urea for all treatments reached equilibrium after 30 min and the degradation efficiencies of urea rose extensively after persulfate was added. Along with the elevation of the persulfate dosage from 0.8 to 2 g L^{-1}, the urea removal efficiency improved proportionally. The highest efficiency in removing urea was 73% at 2 g L^{-1} of persulfate concentration, which rose 6.5-fold compared with SCG-BC adsorption alone. This means that a higher persulfate concentration benefited the generation of larger amounts of reactive radicals. Since persulfate was the source of reactive radicals, a higher persulfate concentration can theoretically produce more reactive radicals. Thus, urea can be degraded by the SCG-BC /persulfate catalytic system. The persulfate radical also played a decisive role in removing urea.

However, when the persulfate concentration exceeded 2 g L^{-1}, the urea degradation efficiency declined to some extent when a larger oxidant dosage was employed. Similar outcomes were documented in other research (Li et al., 2019; Lee et al., 2020b). As reported by these studies, it was caused by the scavenging effect on sulfate with superfluous persulfate. Specifically, functional groups on the surface of SCG-BC (such as -OH, C=O, carboxyl C-O, C=C) may work as catalysts for the electron-transfer mediator and decomposition of PS (Lee et al., 2020b). $SO_4^{\bullet -}$ could be then released immediately with the persulfate decomposition. Excessive $SO_4^{\bullet -}$ might scavenge amongst themselves or consume the remaining persulfate (Lee et al., 2020b), resulting in diminished ability to remove urea (see Eq. (1) and (2)):

$$SO_4^{\bullet -} + SO_4^{\bullet -} \rightarrow S_2O_8^{2-} \quad (1)$$

$$S_2O_8^{2-} + SO_4^{\bullet -} \rightarrow S_2O_8^{\bullet -} + SO_4^{2-} \quad (2)$$

It was presumed that the activation of the sulfate radical activation was primarily attributed to biochar, and some studies have proved that biochar could effectively help produce sulfate radicals (He et al., 2019; Luo et al., 2020; Zhou et al., 2020). Generally, $SO_4^{\bullet -}$ generation during the persulfate activation process was mainly due to the acceptance of electrons from the catalyst to persulfate, which led to cleaving of the -O-O- bond in persulfate (Zhu et al., 2019b). Overall, the capacity of SCG-BC to provide electrons might be explained in two ways. On one hand, the highly graphitized carbon structure of SCG-BC despite its many defects was beneficial to the electron transfer between persulfate and SCG-BC (Zhu et al., 2019b; Luo et al., 2020). On the other hand, oxygen functional groups such as -OH, C=O, and the conjugated aromatic structure (C=C) on the surface of SCG-BC can act as the electron transfer mediator during the persulfate activated process (Wu et al., 2018; Zhang et al., 2020a). To further analyze the possible urea removal pathway, the XPS spectra of SCG-BC before and after reaction were examined. The

detailed analysis is described in more detail in section 3.3.

3.2.3. Effect of SCG-BC dosage

As shown in Fig. 4, the best possible SCG-BC dosage was 0.2 g L^{-1} for activation persulfate to decompose urea. The degradation of urea was enhanced as SCG-BC dosage increased in the 0.05 - 0.2 g L^{-1} range. For instance, approximately 63% of urea was degraded with 0.05 g L^{-1} SCG-BC, whereas about 73% of urea was degraded with 0.2 g L^{-1} SCG-BC, which agrees with other studies (Wu et al., 2018; Ouyang et al., 2019). A higher SCG-BC dosage can encourage more active sites to activate persulfate. However, an excessive SCG-BC dosage (from 0.2 to 0.8 g L^{-1}) caused the urea removal rate to fall to 66%. This is caused by radical–radical reaction as shown in Eq. (1) (Zhu et al., 2019a):

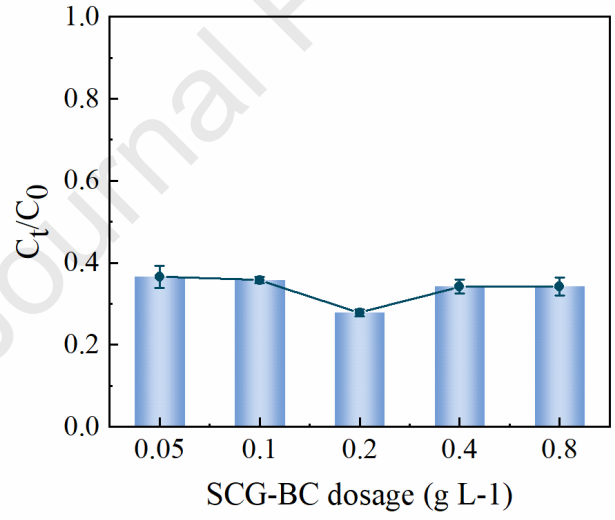

Fig. 4. The effect of SCG-BC dosage in the catalytic system ([persulfate] 2 g L^{-1}, [urea] 1 mg L^{-1}; C_0 represent the initial urea concentration (mg L^{-1}) in the solution; C_t represent the urea concentration (mg L^{-1}) in the solution after the degradation reaction.)

3.2.4. Effect of initial pH on urea removal

pH is an important operating parameter for persulfate activation. The effect of initial solution pH on urea removal was investigated, and the results were shown in Fig. 5. The urea

degradation efficiencies were 60%, 63%, 73% and 61% when the initial pH was 3.0, 5.0, 7.0 and 9.0, respectively. It suggested that initial solution pH had a weak effect on the SCG-BC /persulfate system, so as it could remove urea effectively in a wide pH range (3.0 to 10.0) and the optimum initial pH of the system was at neutral condition. In addition, the initial pH of urea (1 mg L^{-1}) was around 7.0 without pH adjustment, which could reach the best removal effect. It was noticed that after reaction, the final pH value dropped rapidly to 2.87, 3.42, 3.53 and 3.79 when the initial pH were 3.0, 5.0, 7.0 and 9.0, respectively. It was due to the acidification caused by the addition of persulfate (Hu et al., 2020a). In the UPW system, sulfate ions can inevitably be produced when persulfate was used to remove urea in reclaimed water. Therefore, the process should be introduced into the pretreatment stage and sulfate ions can be removed effectively through the subsequent desalination stage. In addition, reducing the dosage of persulfate is also necessary to lower the impact of sulfate ions on UPW system.

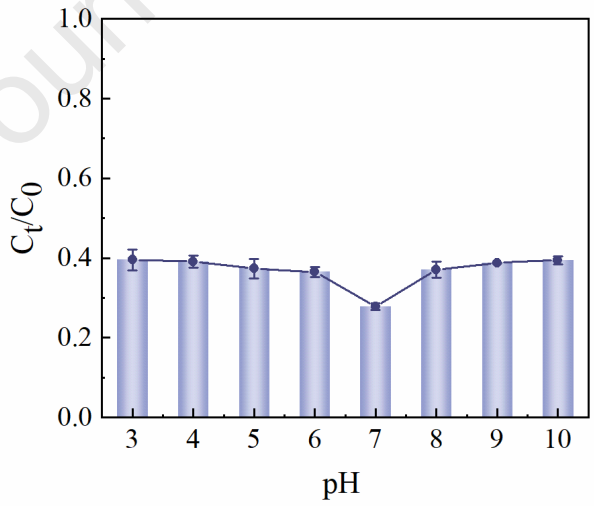

Fig. 5. The effect of pH in the catalytic system ([persulfate] 2 g L^{-1}, [SCG-BC] 0.2 g L^{-1}, [urea] 1 mg L^{-1}; C_0 represent the initial urea concentration (mg L^{-1}) in the solution; C_t represent the urea concentration (mg L^{-1}) in the solution after the degradation reaction.)

3.3. The urea degradation pathway

In order to investigate the degradation mechanism of SCG-BC /persulfate system, it was necessary to determine the radicals produced in the system. According to the relevant reports (Ghauch et al., 2017), MeOH could strongly scavenge $OH^{\bullet}$ and $SO_4^{\bullet -}$, while TBA had high reactivity to $OH^{\bullet}$ and weak reactivity to $SO_4^{\bullet -}$. Therefore, methanol and TBA were selected as quenchers to determine the contribution of radicals in the SCG-BC /persulfate system.

Four systems were used for comparison: System 1 was the control group without quenchers; System 2 was the $OH^{\bullet}$ scavenging system by adding TBA; System 3 was the $OH^{\bullet}$ and $SO_4^{\bullet -}$ scavenging system by adding MeOH; and System 4 was consisted of persulfate only without quenchers and catalysts. When $OH^{\bullet}$ and $SO_4^{\bullet -}$ were removed (system 3), the urea degradation was significantly reduced and could only reach 49% (Fig. 5a). Conversely, after TBA was added, only $SO_4^{\bullet -}$ remained in the urea solution, but the degradation rate can still reach 66%. It was concluded that $SO_4^{\bullet -}$ was the main radical in the SCG-BC /persulfate system.

Fig. 5b presented the contribution of each radical in the urea oxidation process. The best urea degradation rate was 73% without any quenchers. Of note, as the direct oxidation by persulfate was a completely nonradical process without any radicals, the effect of excessive MeOH can be ignored (Ding et al., 2021). Therefore, MeOH quenching experiment showed that 49% of urea degradation was caused by the direct reaction between persulfate and urea. Furthermore, TBA quenching experiment demonstrated that 66% of urea degradation is due to the direct reaction and $SO_4^{\bullet -}$, of which 49% was caused by the direct reaction, and the rest 17% is due to the contribution of $SO_4^{\bullet -}$. However, results showed that the urea degradation rate was 55% when persulfate was added alone. It was speculated that $OH^{\bullet}$ may be produced by

persulfate dissolved in water (see Eq. (3)-(5) (Huang et al., 2021)). Moreover, it can be inferred the contribution of $OH^{\bullet}$ in the catalytic system was weak, only about 1 %, which may be formed by the reaction of $SO_4^{\bullet -}$ with water (Eq. (6) (Ghauch et al., 2017)).

$$S_2O_8^{2-} + H_2O \rightarrow SO_5^{2-} + SO_4^{2-} + 2H^+ \quad (3)$$

$$SO_5^{2-} + H_2O \rightarrow SO_4^{2-} + H_2O_2 \quad (4)$$

$$H_2O_2 \rightarrow 2\ OH^{\bullet} \quad (5)$$

$$SO_4^{\bullet -} + H_2O \rightarrow OH^{\bullet} + HSO_4^- \quad (6)$$

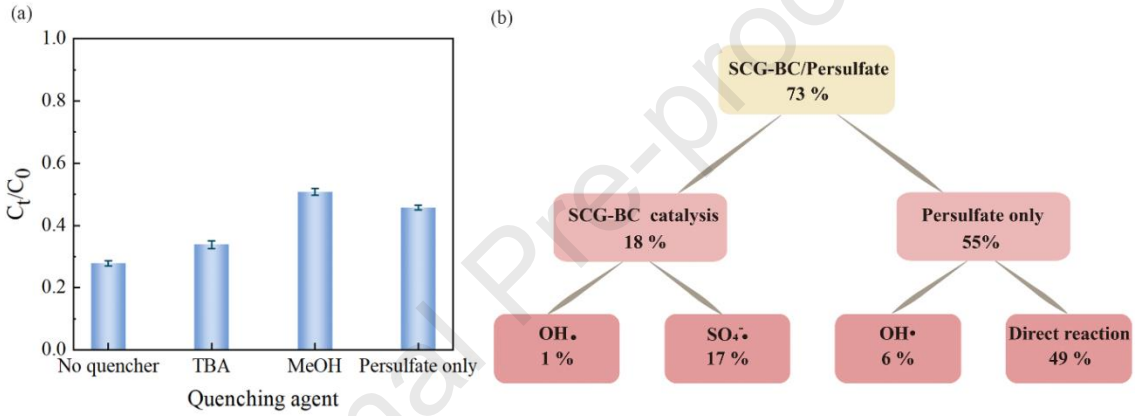

Fig. 6. (a) Effect of MeOH and TBA on urea degradation in SCG-BC /persulfate and in persulfate-only systems; (b) Contribution of each radical.

The possible pathway of urea degradation by catalysis was analyzed and characterized by XPS and FTIR methods. The peaks at around 3441, 1636 and 1380 cm^{-1}, represented the stretching vibration of -OH, C=O or C=C, carboxyl C-O, respectively. The peak vibration intensity at around 3441, 1636 and 1380 cm^{-1} were significantly reduced compared with those before the reaction (Fig. S1). This means that the oxygen functional groups (-OH, C=O, carboxyl C-O) were consumed in the catalytic process, resulting in the weakening of peak vibration intensity. Moreover, the conjugated aromatic structure (C=C) contributed to this process, so these oxygen functional groups and structure may activate the persulfate.

Specifically, they could provide electrons for persulfate, and the persulfate could be activated by accepting electrons from SCG-BC, and in this way the catalytic process worked successfully.

To obtain more detailed information about SCG-BC before and after activation, XPS was used to detect C and O contents (see Supplementary Materials). The characteristic peaks of C1 and O1s were located at around 285 and 533 eV, respectively. After reaction the oxygen content clearly rose and it was attributed to the surface oxidation of SCG-BC. The surface functional groups were oxidized as intermediates in the electron transfer process, thus increasing the oxygen content. Additionally, the surface oxidation of SCG-BC may also result from the highly oxidation-prone environment, which was generated by free radicals during the reaction (Liu et al., 2020).

The C1s spectra in Fig. 7a and 7c exhibited varieties of different functional groups of SCG-BC before and after reaction. Fig. 7a reveals that a wide C1s peak of original SCG-BC consisted of three primary compounds centering at 284.8, 286.1 and 288.1 eV, which were attributed to graphite C/C-C/C-H, C=O and COOH, respectively. For used SCG-BC (Fig. 7c), three main species centering at 284.8, 286.2 and 288.8 eV can also be attributed to graphite C/C-C/C-H, C=O and COOH, respectively (Liu et al., 2020; Zhou et al., 2020). Apparently, the ratio of graphite C (284.8 eV) in SCG-BC was as high as 78.73% but these declined significantly to 55.11% after reaction, while the peaks belonging to C=O (286.1 eV) and COOH (288.1 eV) increased from 15.32%, 5.95% to 32.54% and 12.36%, respectively. Consequently, these results confirmed the transformation of the SCG-BC's surface functional groups. Moreover, graphite C might play a significant role in persulfate activation (see Eq. (7) (Li et al., 2017)):

$$BC\text{-}\pi + S_2O_8^{2-} \rightarrow BC\text{-}\pi^+ + SO_4^{\bullet -} + HSO_4^- \quad (7)$$

In addition, the O1s spectra of SCG-BC are depicted in Fig. 7b and 7d. For pristine SCG-

BC (Fig. 7b), three main species centering at 531.1, 533.0 and 535.8 eV could be attributed to C=O, C-OH/C-O-C and O_2/H_2O, respectively. For used SCG-BC (Fig. 7d), the peak could also fit into the three species, i.e. 531.4, 533.0 and 533.9 eV, performing the stretching vibration of C=O, C-OH/C-O-C and O_2/H_2O, respectively (Zhou et al., 2020). Obviously, the peak assigned to C=O (531.1 eV) dropped from 58.75% to 32.12%, while the peak assigned to C-OH/C-O-C (533.0 eV) increased from 34.91% to 40.70%. These results suggested that these oxygen-containing functional groups, namely C=O and C-OH/C-O-C, all participated in the catalytic process as electron donors and essentially the outcomes are consistent with what FTIR found.

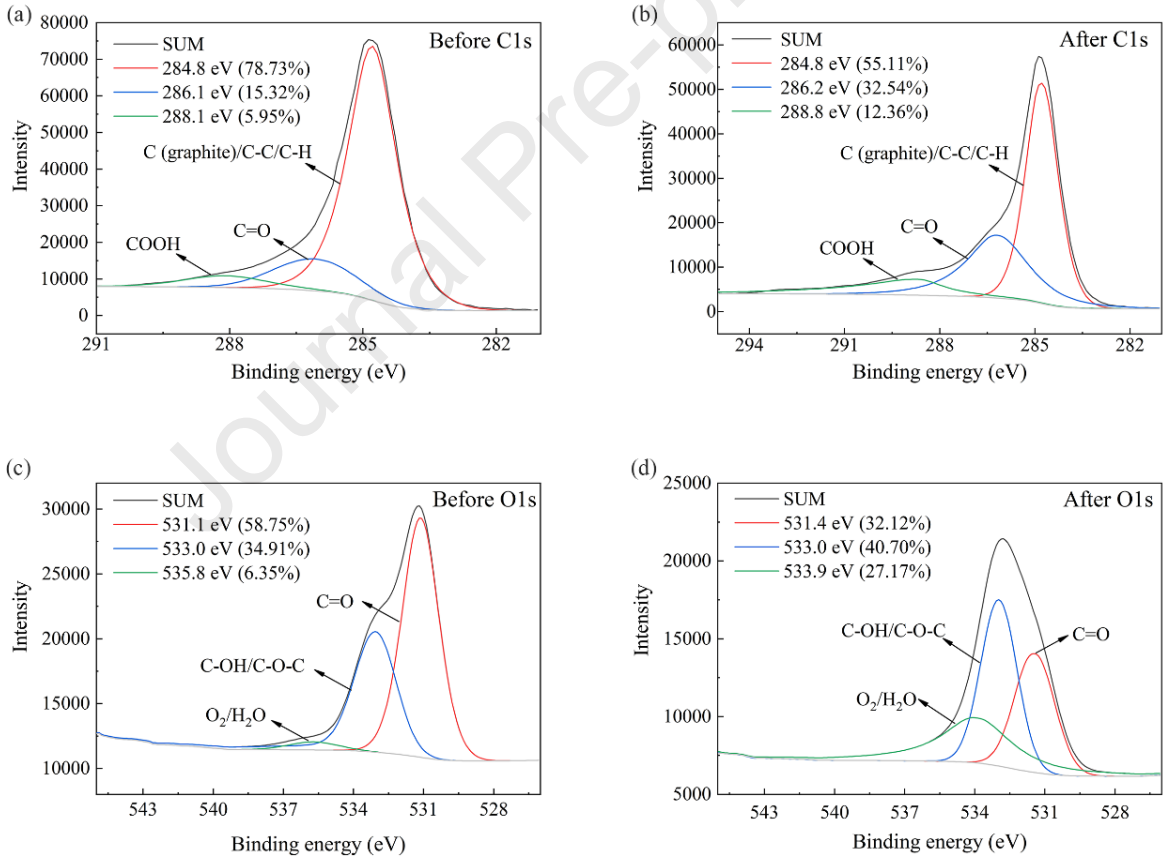

Fig. 7. (a) C1s spectra of SCG-BC before (a) and after (b) reaction; O1s spectra of SCG-BC before (c) and after (d) reaction

Overall, persulfate activation was closely related to these oxygen functional groups and

graphite C. Some studies confirmed that sp^3 carbon is too inactive to decompose persulfate, while sp^2 carbon and oxygen functional groups are responsible for persulfate activation (Duan et al., 2016). In this present study, graphite C might act as an active site to decompose persulfate to form $SO_4^{\bullet -}$ as shown by Eq. (3). Furthermore, the oxygen functional groups (-OH, C=O) played a significant role in the persulfate activation as depicted in Eq. (8) - (9) (Li et al., 2017; Zhu et al., 2019b):

$$BC_{surf} - OH + S_2O_8^{2-} \rightarrow BC_{surf} - O^{\bullet} + SO_4^{\bullet -} + HSO_4^{-} \quad (8)$$

$$BC_{surf} - C{=}O + S_2O_8^{2-} \rightarrow BC_{surf} - C{-}O^{\bullet} + SO_4^{\bullet -} + HSO_4^{-} \quad (9)$$

4. Conclusions

In this work, the introduction of SCG-BC/persulfate process into UPW system was proposed for the first time. It was proved that SCG-BC/persulfate degraded urea in reclaimed water effectively and ensured the UPW effluent quality. Results indicated that SCG-BC can only adsorb small concentrations of urea in water. However, using SCG-BC activating persulfate can greatly improve efficiency in urea decomposition. The oxygen functional groups, graphite C and defect structures in SCG-BC were the essential active centers to activate persulfate and $SO_4^{\bullet -}$ played a vital role on the urea removal in this system. Additionally, the persulfate concentration and SCG-BC dosage were important factors in the SCG-BC /persulfate system. It was discovered that too much persulfate and SCG-BC can undermine the urea removal efficiency. The process could degrade urea effectively in a wide pH range due to slight effect of pH on the catalytic system. To sum up, the SCG-BC /persulfate system is a promising option for efficient urea removal in the UPW production system. In view of the complexity of the actual reclaimed water and diversity of carbon-based catalysts, further studies on

409 competitive adsorption and other carbon-based catalysts must be urgently undertaken.

410

411 **Acknowledgements**

412 This research was supported by Tianjin Municipal Science and Technology Bureau of
413 China (Project No. 18PTZWHZ00140, 20JCZDJC00380) and TG Hilyte Environment
414 Technology (Beijing) Co., LTD. (Project No. M-P-0-181001-001).

415

416

417 **References**

418 Ahmad, M., Rajapaksha, A.U., Lim, J.E., Zhang, M., Bolan, N., Mohan, D., Vithanage,
419 M., Lee, S.S., Ok, Y.S., 2014. Biochar as a sorbent for contaminant management in soil and
420 water: a review. Chemosphere 99, 19-33.

421 Al Hakim, S., Baalbaki, A., Tantawi, O., Ghauch, A., 2019. Chemically and thermally
422 activated persulfate for theophylline degradation and application to pharmaceutical factory
423 effluent. RSC Adv. 9, 33472-33485.

424 Al Hakim, S., Jaber, S., Zein Eddine, N., Baalbaki, A., Ghauch, A., 2020. Degradation of
425 theophylline in a UV254/PS system: matrix effect and application to a factory effluent. Chem.
426 Eng. J. 380, 122478.

427 ASTM, 2018. Standard guide for ultra-pure water wsed in the electronics and
428 semiconductor industries (ASTM D5127-13(2018)). American Society of Testing and
429 Materials International, West Conshohocken, PA.

430 Chen, X., Oh, W.-D., Lim, T.-T., 2018. Graphene- and CNTs-based carbocatalysts in
431 persulfates activation: material design and catalytic mechanisms. Chem. Eng. J. 354, 941-976.

Cheng, X., Guo, H., Zhang, Y., Wu, X., Liu, Y., 2017. Non-photochemical production of singlet oxygen via activation of persulfate by carbon nanotubes. Water Res. 113, 80-88.

Choi, J., Chung, J., 2019. Evaluation of urea removal by persulfate with UV irradiation in an ultrapure water production system. Water Res. 158, 411-416.

Choi, J., Kim, J.-O., Chung, J., 2016. Removal of isopropyl alcohol and methanol in ultrapure water production system using a 185 nm ultraviolet and ion exchange system. Chemosphere 156, 341-346.

Clurman, A.M., Rodríguez-Narvaez, O.M., Jayarathne, A., De Silva, G., Ranasinghe, M.I., Goonetilleke, A., Bandala, E.R., 2020. Influence of surface hydrophobicity/hydrophilicity of biochar on the removal of emerging contaminants. Chem. Eng. J. 402, 126277.

Ding, Y., Wang, X., Fu, L., Peng, X., Pan, C., Mao, Q., Wang, C., Yan, J., 2021. Nonradicals induced degradation of organic pollutants by peroxydisulfate (PDS) and peroxymonosulfate (PMS): recent advances and perspective. Sci. Total Environ. 765, 142794.

Dong, C.-D., Chen, C.-W., Hung, C.-M., 2017. Synthesis of magnetic biochar from bamboo biomass to activate persulfate for the removal of polycyclic aromatic hydrocarbons in marine sediments. Bioresour. Technol. 245, 188-195.

Duan, X., Su, C., Miao, J., Zhong, Y., Shao, Z., Wang, S., Sun, H., 2018. Insights into perovskite-catalyzed peroxymonosulfate activation: maneuverable cobalt sites for promoted evolution of sulfate radicals. Appl. Catal. B Environ. 220, 626-634.

Duan, X., Sun, H., Ao, Z., Zhou, L., Wang, G., Wang, S., 2016. Unveiling the active sites of graphene-catalyzed peroxymonosulfate activation. Carbon 107, 371-378.

Dutta, S., Bhaumik, A., Wu, K.C.W., 2014. Hierarchically porous carbon derived from

polymers and biomass: effect of interconnected pores on energy applications. Energy Environ. Sci. 7, 3574-3592.

Ferrari, A.C., Robertson, J., 2000. Interpretation of raman spectra of disordered and amorphous carbon. Phys. Rev. B 61, 14095-14107.

Ghauch, A., Baalbaki, A., Amasha, M., El Asmar, R., Tantawi, O., 2017. Contribution of persulfate in UV-254nm activated systems for complete degradation of chloramphenicol antibiotic in water. Chem. Eng. J. 317, 1012-1025.

Guizani, C., Haddad, K., Limousy, L., Jeguirim, M., 2017. New insights on the structural evolution of biomass char upon pyrolysis as revealed by the raman spectroscopy and elemental analysis. Carbon 119, 519-521.

Guo, T., Englehardt, J., Wu, T., 2014. Review of cost versus scale: water and wastewater treatment and reuse processes. Water Sci. Technol. 69, 223-234.

He, J., Xiao, Y., Tang, J., Chen, H., Sun, H., 2019. Persulfate activation with sawdust biochar in aqueous solution by enhanced electron donor-transfer effect. Sci. Total Environ. 690, 768-777.

Hu, P., Long, M., 2016. Cobalt-catalyzed sulfate radical-based advanced oxidation: a review on heterogeneous catalysts and applications. Appl. Catal. B Environ. 181, 103-117.

Hu, W., Tong, W., Li, Y., Xie, Y., Chen, Y., Wen, Z., Feng, S., Wang, X., Li, P., Wang, Y., Zhang, Y., 2020a. Hydrothermal route-enabled synthesis of sludge-derived carbon with oxygen functional groups for bisphenol A degradation through activation of peroxymonosulfate. J. Hazard. Mater. 388, 121801.

Hu, X., Zhang, X., Ngo, H.H., Guo, W., Wen, H., Li, C., Zhang, Y., Ma, C., 2020b. Comparison study on the ammonium adsorption of the biochars derived from different kinds

478 of fruit peel. Sci. Total Environ. 707, 135544.

479 Huang, W., Xiao, S., Zhong, H., Yan, M., Yang, X., 2021. Activation of persulfates by
480 carbonaceous materials: a review. Chem. Eng. J. 418, 129297.

481 Huggins, T.M., Haeger, A., Biffinger, J.C., Ren, Z.J., 2016. Granular biochar compared
482 with activated carbon for wastewater treatment and resource recovery. Water Res. 94, 225-
483 232.

484 Keiluweit, M., Nico, P.S., Johnson, M.G., Kleber, M., 2010. Dynamic molecular
485 structure of plant biomass-derived black carbon (biochar). Environ. Sci. Technol. 44, 1247-
486 1253.

487 Lee, J., von Gunten, U., Kim, J.-H., 2020a. Persulfate-based advanced oxidation: critical
488 assessment of opportunities and roadblocks. Environ. Sci. Technol. 54, 3064-3081.

489 Lee, Y.-C., Li, Y.-f., Chen, M.-J., Chen, Y.-C., Kuo, J., Lo, S.-L., 2020b. Efficient
490 decomposition of perfluorooctanic acid by persulfate with iron-modified activated carbon.
491 Water Res. 174, 115618.

492 Lefebvre, O., 2018. Beyond NEWater: an insight into Singapore's water reuse prospects.
493 Current Opinion in Environmental Science & Health 2, 26-31.

494 Li, F., Xie, Y., Wang, Y., Fan, X., Cai, Y., Mei, Y., 2019. Improvement of dyes
495 degradation using hydrofluoric acid modified biochar as persulfate activator. Environ. Pollut.
496 Bioavailability 31, 32-37.

497 Li, J., Lin, H., Zhu, K., Zhang, H., 2017. Degradation of acid orange 7 using
498 peroxymonosulfate catalyzed by granulated activated carbon and enhanced by electrolysis.
499 Chemosphere 188, 139-147.

500 Liang, J., Xu, X., Qamar Zaman, W., Hu, X., Zhao, L., Qiu, H., Cao, X., 2019. Different

mechanisms between biochar and activated carbon for the persulfate catalytic degradation of sulfamethoxazole: roles of radicals in solution or solid phase. Chem. Eng. J. 375, 121908.

Liu, H., Liu, Y., Tang, L., Wang, J., Yu, J., Zhang, H., Yu, M., Zou, J., Xie, Q., 2020. Egg shell biochar-based green catalysts for the removal of organic pollutants by activating persulfate. Sci. Total Environ. 745, 141095.

Liu, L., Lin, Y., Liu, Y., Zhu, H., He, Q., 2013. Removal of methylene blue from aqueous solutions by sewage sludge based granular activated carbon: adsorption equilibrium, kinetics, and thermodynamics. J. Chem. Eng. Data 58, 2248-2253.

Luo, J., Bo, S., Qin, Y., An, Q., Xiao, Z., Zhai, S., 2020. Transforming goat manure into surface-loaded cobalt/biochar as PMS activator for highly efficient ciprofloxacin degradation. Chem. Eng. J. 395, 125063.

Mortazavian, S., Jones-Lepp, T., Bae, J.-H., Chun, D., Bandala, E.R., Moon, J., 2019. Heat-treated biochar impregnated with zero-valent iron nanoparticles for organic contaminants removal from aqueous phase: material characterizations and kinetic studies. J. Ind. Eng. Chem. 76, 197-214.

Nguyen, C.H., Fu, C.-C., Chen, Z.-H., Tran, T.T.V., Liu, S.-H., Juang, R.-S., 2021. Enhanced and selective adsorption of urea and creatinine on amine-functionalized mesoporous silica SBA-15 via hydrogen bonding. Microporous Mesoporous Mater. 311, 110733.

Nguyen, V.-T., Nguyen, T.-B., Chen, C.-W., Hung, C.-M., Huang, C.P., Dong, C.-D., 2019a. Cobalt-impregnated biochar (Co-SCG) for heterogeneous activation of peroxymonosulfate for removal of tetracycline in water. Bioresour. Technol. 292, 121954.

Nguyen, V.-T., Nguyen, T.-B., Chen, C.-W., Hung, C.-M., Vo, T.-D.-H., Chang, J.-H.,

Dong, C.-D., 2019b. Influence of pyrolysis temperature on polycyclic aromatic hydrocarbons production and tetracycline adsorption behavior of biochar derived from spent coffee ground. Bioresour. Technol. 284, 197-203.

Oh, W.-D., Dong, Z., Lim, T.-T., 2016. Generation of sulfate radical through heterogeneous catalysis for organic contaminants removal: current development, challenges and prospects. Appl. Catal. B Environ. 194, 169-201.

Oleszczuk, P., Godlewska, P., Reible, D.D., Kraska, P., 2017. Bioaccessibility of polycyclic aromatic hydrocarbons in activated carbon or biochar amended vegetated (salix viminalis) soil. Environ. Pollut. 227, 406-413.

Ouyang, D., Chen, Y., Yan, J., Qian, L., Han, L., Chen, M., 2019. Activation mechanism of peroxymonosulfate by biochar for catalytic degradation of 1,4-dioxane: important role of biochar defect structures. Chem. Eng. J. 370, 614-624.

Ren, W., Xiong, L., Yuan, X., Yu, Z., Zhang, H., Duan, X., Wang, S., 2019. Activation of peroxydisulfate on carbon nanotubes: electron-transfer mechanism. Environ. Sci. Technol. 53, 14595-14603.

Rydzewski, J., Godec, R., 2002. Undetectable TOC in UPW can influence DUV photolithography processes. Semiconductor Pure Water and Chemicals Conference, pp. 30-48.

Schmotzer, M., Castro, M., Shadman, F., 2002. Activated carbon removal of organic contaminants in ultra-pure water systems with recycle. Clean Techn. Environ. Policy 4, 125-132.

Shao, P., Tian, J., Yang, F., Duan, X., Gao, S., Shi, W., Luo, X., Cui, F., Luo, S., Wang, S., 2018. Identification and regulation of active sites on nanodiamonds: establishing a highly

efficient catalytic system for oxidation of organic contaminants. Advanced Functional Materials 28, 1705295.

Singh, R., 2016. Chapter 13 - Development of hybrid processes for high purity water production. in: Hankins, N.P., Singh, R. (Eds.). Emerging Membrane Technology for Sustainable Water Treatment. Elsevier, Boston, pp. 327-357.

Sun, T., Chen, K., 2014. Removal of isopropyl alcohol (IPA) in UPW by synergistic photocatalytic oxidation and adsorption. Can. J. Chem. Eng. 92, 1174-1180.

Wang, H., Maiyalagan, T., Wang, X., 2012. Review on recent progress in nitrogen-doped graphene: synthesis, characterization, and its potential applications. ACS Catal. 2, 781-794.

Wang, S., Liu, H., Gu, J., Sun, H., Zhang, M., Liu, Y., 2019. Technology feasibility and economic viability of an innovative integrated ceramic membrane bioreactor and reverse osmosis process for producing ultrapure water from municipal wastewater. Chem. Eng. J. 375, 122078.

Wu, Y., Guo, J., Han, Y., Zhu, J., Zhou, L., Lan, Y., 2018. Insights into the mechanism of persulfate activated by rice straw biochar for the degradation of aniline. Chemosphere 200, 373-379.

Xiu, S., Shahbazi, A., Li, R., 2017. Characterization, modification and application of biochar for energy storage and catalysis: a review. Trends in Renewable Energy 3, 86-101.

Xu, X., Zhao, Y., Sima, J., Zhao, L., Mašek, O., Cao, X., 2017. Indispensable role of biochar-inherent mineral constituents in its environmental applications: a review. Bioresour. Technol. 241, 887-899.

Yang, Y., Banerjee, G., Brudvig, G.W., Kim, J.-H., Pignatello, J.J., 2018. Oxidation of organic compounds in water by unactivated peroxymonosulfate. Environ. Sci. Technol. 52,

5911-5919.

Yao, B., Luo, Z., Yang, J., Zhi, D., Zhou, Y., 2021a. FeIIFeIII layered double hydroxide modified carbon felt cathode for removal of ciprofloxacin in electro-Fenton process. Environ. Res. 197, 111144.

Yao, B., Luo, Z., Zhi, D., Hou, D., Luo, L., Du, S., Zhou, Y., 2021b. Current progress in degradation and removal methods of polybrominated diphenyl ethers from water and soil: a review. J. Hazard. Mater. 403, 123674.

Yoon, Y., Lueptow, R.M., 2005. Removal of organic contaminants by RO and NF membranes. J. Membr. Sci. 261, 76-86.

Yu, J., Tang, L., Pang, Y., Zeng, G., Wang, J., Deng, Y., Liu, Y., Feng, H., Chen, S., Ren, X., 2019. Magnetic nitrogen-doped sludge-derived biochar catalysts for persulfate activation: internal electron transfer mechanism. Chem. Eng. J. 364, 146-159.

Zhang, H., Xiao, R., Li, R., Ali, A., Chen, A., Zhang, Z., 2020a. Enhanced aqueous Cr(VI) removal using chitosan-modified magnetic biochars derived from bamboo residues. Chemosphere 261, 127694.

Zhang, X., Yang, Y., Ngo, H.H., Guo, W., Wen, H., Wang, X., Zhang, J., Long, T., 2021. A critical review on challenges and trend of ultrapure water production process. Sci. Total Environ. 785, 147254.

Zhang, X., Zhang, Y., Ngo, H.H., Guo, W., Wen, H., Zhang, D., Li, C., Qi, L., 2020b. Characterization and sulfonamide antibiotics adsorption capacity of spent coffee grounds based biochar and hydrochar. Sci. Total Environ. 716, 137015.

Zhao, P., Bai, Y., Liu, B., Chang, H., Cao, Y., Fang, J., 2019. Process optimization for producing ultrapure water with high resistivity and low total organic carbon. Process Saf.

593 Environ. Prot. 126, 232-241.

594 Zhou, X., Zeng, Z., Zeng, G., Lai, C., Xiao, R., Liu, S., Huang, D., Qin, L., Liu, X., Li,
595 B., Yi, H., Fu, Y., Li, L., Wang, Z., 2020. Persulfate activation by swine bone char-derived
596 hierarchical porous carbon: multiple mechanism system for organic pollutant degradation in
597 aqueous media. Chem. Eng. J. 383, 123091.

598 Zhu, K., Wang, X., Chen, D., Ren, W., Lin, H., Zhang, H., 2019a. Wood-based biochar as
599 an excellent activator of peroxydisulfate for acid orange 7 decolorization. Chemosphere 231,
600 32-40.

601 Zhu, K., Wang, X., Geng, M., Chen, D., Lin, H., Zhang, H., 2019b. Catalytic oxidation
602 of clofibric acid by peroxydisulfate activated with wood-based biochar: effect of biochar
603 pyrolysis temperature, performance and mechanism. Chem. Eng. J. 374, 1253-1263.